

## Chopper system for time resolved experiments with synchrotron radiation

Marco Cammarata,<sup>1</sup> Laurent Eybert,<sup>1</sup> Friederike Ewald,<sup>1</sup> Wolfgang Reichenbach,<sup>1</sup> Michael Wulff,<sup>1,a)</sup> Philip Anfinrud,<sup>2</sup> Friedrich Schotte,<sup>2</sup> Anton Plech,<sup>3</sup> Qingyu Kong,<sup>4</sup> Maciej Lorenc,<sup>5</sup> Bernd Lindenau,<sup>6</sup> Jürgen Rübiger,<sup>6</sup> and Stephan Polachowski<sup>6</sup>

<sup>1</sup>European Synchrotron Radiation Facility, BP 220, Grenoble Cedex 38043, France

<sup>2</sup>Laboratory of Chemical Physics, National Institutes of Health, Bethesda, Maryland 20892-0520, USA

<sup>3</sup>Institute for Synchrotron Radiation (ISS), FZ Karlsruhe, Postfach 3640, D-76021 Karlsruhe, Germany

<sup>4</sup>Synchrotron SOLEIL, Saint-Aubin, 91192 Gif-sur-Yvette, France

<sup>5</sup>Groupe Matière Condensée et Matériaux, Université de Rennes 1, UMR6626 CNRS, 35042 Rennes Cedex, France

<sup>6</sup>Central Technology Division (ZAT), Forschungszentrum Jülich GmbH, Leo-Brandt-Str., 52425 Jülich, Germany

(Received 3 July 2008; accepted 4 November 2008; published online 6 January 2009)

A chopper system for time resolved pump-probe experiments with x-ray beams from a synchrotron is described. The system has three parts: a water-cooled heatload chopper, a high-speed chopper, and a millisecond shutter. The chopper system, which is installed in beamline ID09B at the European Synchrotron Radiation Facility, provides short x-ray pulses for pump-probe experiments with ultrafast lasers. The chopper system can produce x-ray pulses as short as 200 ns in a continuous beam and repeat at frequencies from 0 to 3 kHz. For bunch filling patterns of the synchrotron with pulse separations greater than 100 ns, the high-speed chopper can isolate single 100 ps x-ray pulses that are used for the highest time resolution. A new rotor in the high-speed chopper is presented with a single pulse (100 ps) and long pulse (10  $\mu$ s) option. In white beam experiments, the heatload of the (noncooled) high-speed chopper is lowered by a heatload chopper, which absorbs 95% of the incoming power without affecting the pulses selected by the high speed chopper. © 2009 American Institute of Physics. [DOI: 10.1063/1.3036983]

### I. INTRODUCTION

It has always been a dream to visualize the structure of molecules in chemical and biochemical reactions with x rays, but that has so far been difficult to do due to the short times involved and the relatively low pulse intensity of state-of-the-art x-ray sources. Bond formation, isomerization, and electron transfer are fundamental chemical steps that evolve on the femtosecond and picosecond time scales and ultrafast techniques are therefore needed to probe molecules in time. Three pump-probe techniques are currently used and all use short optical pulses to initiate and clock the reaction. The probe pulse is then either an optical pulse, an electron pulse, or an x-ray pulse. X rays are particularly powerful for structural work since their wavelengths match atom-atom distances in molecules and they can penetrate condensed samples much deeper than electrons. With the advent of third generation synchrotrons such as the European Synchrotron Radiation Facility (ESRF), pulsed quasimonochromatic beams of hard x rays are now available with a pulse length of around 100 ps and with  $10^9$  to  $10^{10}$  photons/pulse. By varying the delay between the laser and the x-ray pulse, scattering patterns can be collected as a function of delay with each delay being a 100 ps snapshot of the moving molecular structure. Protein dynamics has been filmed in crystals<sup>1-4</sup> and more recently in solution<sup>5</sup> and that has deepened our understanding of how the function of a protein is related to its time

dependent structure. Another new field is dissociation and recombination dynamics of small molecules in solution,<sup>6-9</sup> where transient structures of the molecules and their surrounding medium can be studied in great detail.<sup>10,11</sup>

The most efficient way to conduct a time resolved experiment is to film it, i.e., initiate a given reaction and then open an x-ray shutter, and record the change in the scattered x rays as a function of time. Unfortunately the time resolution of area detectors is milliseconds at best, i.e.,  $10^7$  times longer than the x-ray pulse. To exploit the single-pulse resolution of a synchrotron, multiple scattering patterns from a fixed laser/x-ray delay have to be accumulated in the detector, which slows down the speed of the data acquisition considerably. The frequency of a pump-probe experiment might vary from single-shot data acquisition in protein crystallography (0 Hz) to 3 kHz in flow cell experiments where the sample is replaced at high speed. Note that the chopper system is designed not only to produce short x-ray pulses but also to slow down the x-ray frequency to a usable level for a given sample.

The first high-speed chopper for synchrotrons was designed in 1988 by Wilfried Schildkamp and Claude Praderwand, University of Chicago, and used at Chess for the first single-pulse Laue experiments on lysozyme crystals.<sup>12</sup> The beam was chopped by two slits in a rotating disk with mechanical bearings. An upgraded version of this design was later used at ESRF in single pulse experiments in 1994.<sup>13</sup> In parallel Kosciesza and Bartunik<sup>14</sup> selected single pulses with a rotating mirror at Desy and McPherson *et al.*<sup>15,16</sup> designed a chopper and a rotating crystal for the Advanced Photon

<sup>a)</sup> Author to whom correspondence should be addressed. Electronic mail: wulff@esrf.fr.

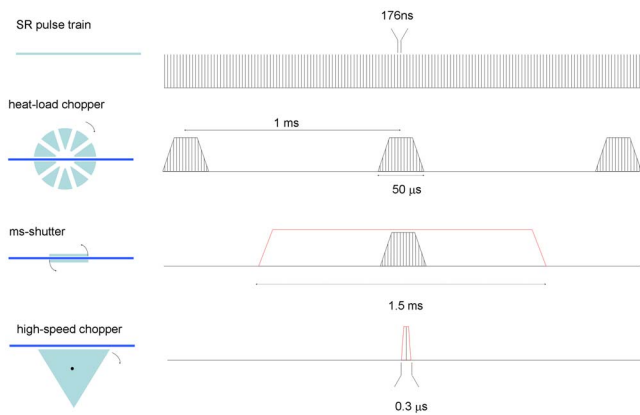


FIG. 1. (Color online) Scheme to isolate single x-ray pulses. When operated in 16-bunch mode, the ESRF produces a train of  $\sim 100$  ps x-ray pulses separated by 176 ns. This pulse train is first chopped by the heatload chopper into  $50 \mu\text{s}$  (FWHM) macrobunches at 1 kHz, thereby reducing by a factor of 20 the transmitted average power striking the x-ray focusing mirror and other downstream components. The millisecond shutter opens on demand to isolate one heatload chopper macrobunch from the 1 kHz train of bunches. The high-speed chopper isolates a single pulse from the center of the transmitted macrobunch.

Source (APS). Rotating mirrors and crystals can produce submicrosecond opening times but the beam position is sensitive to jitter in the rotation speed. A slot-based high-speed chopper rotating in helium with air bearings and vacuum windows was built by Gembicky *et al.*<sup>17</sup> for the ChemMat beamline 15 at the APS. Rotating a 140 mm radius disk with 45 slits (0.35 mm opening) at 502.9 Hz, they produced  $2.1 \mu\text{s}$  open windows for single-pulse beam at APS at a record frequency of 22.6 kHz. They later added a heatload chopper based on the same technology.<sup>18</sup> Note finally that the ESRF triangular chopper design described below is also used on the BioCars beamline 14 at APS, at Spring8, and at KEK.<sup>19</sup>

The ESRF chopper system has three components. In downstream order they are: a heatload chopper in the optics hutch, a millisecond shutter, and high-speed chopper in the experimental hutch near the sample. In the original design, the heatload on the high-speed chopper was reduced by a 5 Hz heatload shutter in the optics hutch, which made white beam experiments rather inefficient.<sup>20–22</sup> In the upgraded system presented here, the heatload shutter is replaced by a 1 kHz heatload chopper and the previous 1 kHz high-speed chopper is upgraded with a 1 kHz microsecond mode ( $10 \mu\text{s}$ ) and a 3 kHz mode.

The timing of the chopper system is shown in Fig. 1 for a single pulse experiment. The 300 ns open window from the high-speed chopper picks out a single pulse from the  $\sim 50 \mu\text{s}$  pulse from the heatload chopper. Both pulses repeat at 1 kHz, so a millisecond shutter is needed to isolate one single pulse. The heatload chopper is placed 29.5 m from the x-ray source in front of the monochromator and the focusing mirror. The heatload is reduced by a factor of  $\sim 20$ , which means that the full peak power of the undulator can be used without overheating the high-speed chopper. The high-speed chopper is placed 53 m from the source in the (quasi) focused beam 1.2 m from the sample. By default, both choppers produce pulses at 986.3 Hz synchronized to the radio

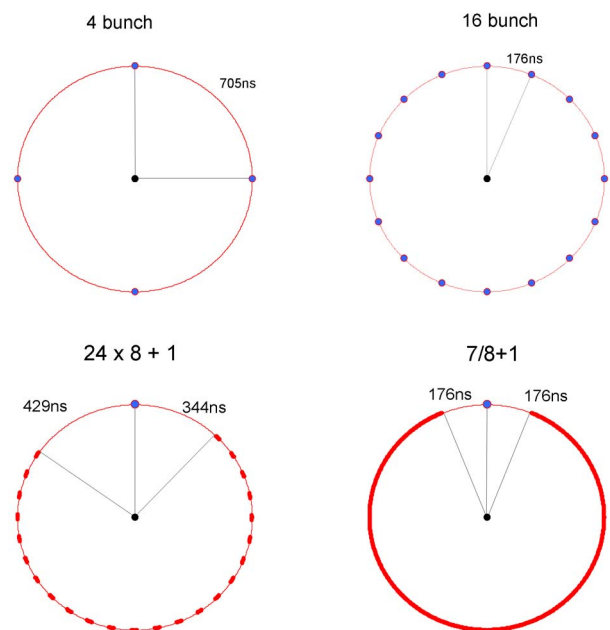


FIG. 2. (Color online) Filling patterns suitable for single-pulse pump-probe experiments at the ESRF: 4-bunch mode (40 mA), 16-bunch mode (90 mA), hybrid mode ( $24 \times 8 + 1$ , 200 mA), and 7/8 mode (200 mA).

frequency (rf) clock of the synchrotron. The millisecond shutter is used to either gate the detector during readout or to produce subharmonics of the high-speed chopper at frequencies up to 80 Hz.

## II. BUNCH MODES FOR SINGLE-PULSE EXPERIMENTS

To exploit the 100 ps time resolution from a single x-ray pulse, the filling pattern of the storage ring has to provide a sufficiently wide time gap for the high-speed chopper to select a single pulse. With present chopper technology and beam sizes, the single pulse has to be separated by at least 100 ns from side pulses for the chopper to eliminate them. At the ESRF there are currently four modes for single pulse experiments: the 4-bunch and 16-bunch mode with equidistant bunch fillings, the hybrid mode, and the 7/8 multibunch mode. These modes run 80% of the time with 20% in uniform mode. We will now shortly describe these bunch modes in detail.

It takes a 6 GeV electron  $2.81657 \mu\text{s}$  to traverse the 844.39 m long synchrotron at ESRF. That corresponds to an orbit frequency of 355.042 kHz. The energy lost to synchrotron radiation is compensated by rf cavities that operate at 352.201 664 MHz, the 992nd harmonic of the orbit frequency. The rf cavities can support up to 992 bunches in a (quasi) uniform fill with pulse separations of 2.839 ns. That time gap is too small for mechanical single pulse isolation, so the shortest achievable pulse is 200 ns given by the mechanical opening. The single-pulse modes are shown in Fig. 2. The time gaps in the 4-bunch and 16-bunch modes are 704 and 176 ns, respectively. In the hybrid mode, the time gaps are slightly asymmetric, 429 and 344 ns. Finally the 7/8 mode has a 352 ns gap with a single bunch in the middle. The low bunch charge in the 7/8 mode, 2.5–5.0 nC, shortens the x-ray pulse to 60–80 ps [full width at half maximum

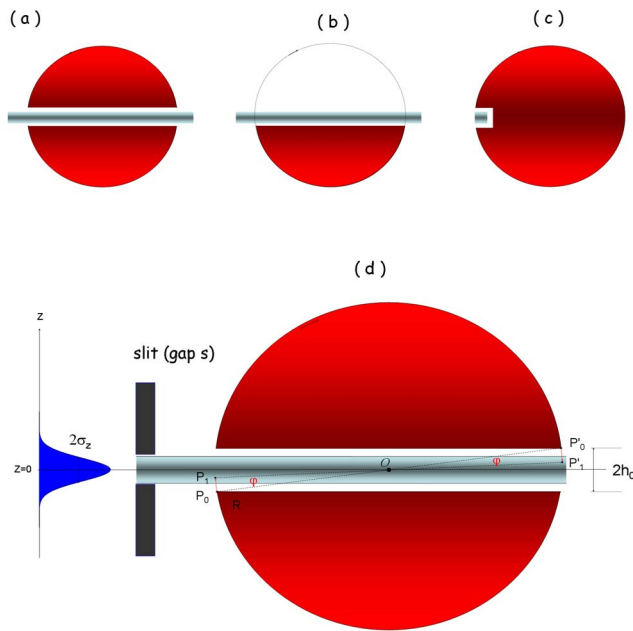


FIG. 3. (Color online) Rotor geometries employed in three classes of choppers: (a) the tunnel chopper, (b) the tunnel-less chopper, and (c) the slotted chopper. The geometrical parameters relevant for computing the time-dependent transmission of a Gaussian beam through a rotating tunnel are shown in (d).

(FWHM)]. For time resolved experiments over wide time ranges, the 7/8 mode offers the advantage that for time delays greater than  $\sim 1 \mu\text{s}$ ; the intensity of the pulse can be boosted by changing the chopper phase by  $180^\circ$ .

### III. THEORETICAL OPEN PROFILES FOR A CHOPPED BEAM

Before discussing the choppers in detail, we will calculate the open profiles for a Gaussian beam for the three main geometries shown in Fig. 3. In the first case [Fig. 3(a)] the beam is chopped by a tunnel in the center of a disk with the rotation axis perpendicular to the beam. This tunnel geometry offers short open times as the beam is cut from above and below simultaneously during the close/open/close cycle by the four end-points. The second case is the tunnel-less chopper where the tunnel ceiling is removed [see Fig. 3(b)]. The beam is cut by one edge at a time, which typically doubles the open time compared to a tunnel. However in the tunnel-less case, the open time can be varied without changing the speed of the chopper by varying the chopper-to-beam distance. In the third type, the slot chopper in Fig. 3(c), the beam passes through slots at the periphery of the disk with the beam parallel to the rotation axis. Having  $N$  equidistant slots around the periphery, the x-ray frequency is  $N$  times the rotation frequency, which is the simplest way to increase the frequency of the pulse train.

#### A. Tunnel-based chopping

We will now calculate the open profile  $I(t)$  for a rotating tunnel, i.e., the time dependent spatially integrated intensity for a close/open/close cycle in a continuous wave (cw) beam. Let  $R$  be the disk radius,  $2h_0$  the height of the tunnel, and  $f$  the rotation frequency. The tunnel is assumed to be small,

$2h_0 \ll R$ , and passing through the center of the disk. The velocity of the cutting edges in the tunnel is perpendicular to the incident beam and  $v = 2\pi fR$ . The incoming beam defines the  $x$ -axis, the  $y$ -axis is the rotation axis, and the beam is cut in the  $z$ -direction. Let's assume a Gaussian beam intensity centered on  $z=0$ ,

$$f(z) = \frac{1}{\sqrt{2\pi}\sigma} \exp\left(-\frac{z^2}{2\sigma^2}\right), \quad (1)$$

where  $\sigma$  is the (rms) beam size in the chopper (FWHM  $= 2(2 \ln 2)^{1/2} \sigma \approx 2.355\sigma$ ). When the tunnel rotates through a close/open/close cycle, the four tunnel edges form a slit, which opens and closes symmetrically around the beam [see Fig. 3(d)]. When the chopper rotates clockwise away from its fully open position, the cutting points  $P_0$  and  $P'_0$  will move to  $P_1$  and  $P'_1$ , while reducing the aperture from above and below symmetrically. When  $h \ll R$  we have

$$h(t) \cong h_0 - |\varphi(t)|R = h_0 - \omega R|t| = h_0 - 2\pi fR|t| \quad (2)$$

for times  $|t| \leq t_0 = h_0 / (2\pi fR)$  and  $h(t) = 0$  for  $|t| > t_0$ . Note that  $t_0 = h_0/v$  where  $v$  is the speed of the disk. The transmitted intensity, integrated in the vertical direction, is the slit integral

$$I(t) \cong \int_{-h(t)}^{h(t)} f(z) dz = \text{erf}\left(\frac{h(t)}{\sqrt{2}\sigma}\right) = \text{erf}\left(\frac{h_0 - 2\pi fR|t|}{\sqrt{2}\sigma}\right), \quad (3)$$

where erf is the error function.

The aperture  $2h(t)$  and intensity  $I(t)$  functions are shown in Figs. 4(a) and 4(b). The intensity is zero outside  $(-t_0, t_0)$ . The total open time, i.e. the base line of the open window is

$$\Delta t_{\text{base}} = 2t_0 = \frac{2h_0}{2\pi fR}, \quad (4)$$

which is the time it takes for a cutting edge on the periphery to move the distance  $2h_0$ . With typical parameters  $h_0 = 0.075 \text{ mm}$ ,  $f = 1000 \text{ Hz}$ , and  $R = 100 \text{ mm}$ , we get  $\Delta t_{\text{base}} = 239 \text{ ns}$ . The tip velocity is  $v = 628.3 \text{ m/s}$ , which is greater than the speed of sound in air ( $343.6 \text{ m/s}$ ). That implies that the disk has to rotate in vacuum suspended in magnetic bearings.

With a tunnel-to-beam-ratio  $h_0/\sigma$  of 1, the open profile is triangular with a peak intensity of  $\sim 0.7$  at the center of the window, whereas for  $h_0/\sigma$  between 3 and 4, there is a plateau at the center with full transmittance. In single pulse experiments, this "top line" is a buffer for rotation jitter. The top line has to be much greater than the timing jitter to avoid cutting the single pulse when the open window arrives slightly early or late. If a pulse arrives in the rising or falling-edge zone, the beam size and the intensity are reduced. In a cw beam, a (small) fraction of the transmitted beam is reflected in the tunnel ceiling and floor, which degrades the collimation and spectra purity (pink beam). This parasitic scattering is readily removed by a collimator near the sample. If the incoming or outgoing beam is reduced in size by a slit  $s \leq 2h_0$ , the central part of the open profile is re-

duced to a constant value, the integral of the beam through the slit,  $\text{erf}[s/2/(\sqrt{2}\sigma)]$ , whereas the rising and falling edges are unchanged.

If the tunnel is placed off-center in the disk, the speed term  $2\pi fR$  in Eqs. (2) and (4) should be replaced with the speed perpendicular to the tunnel when it is open. For the triangular rotor used on beamline ID09B the perpendicular speed is  $\sqrt{3}\pi fR$ .

## B. Tunnel-less based chopping

If the ceiling in the tunnel is removed as shown in Fig. 3(b), the lower limit in the intensity integral becomes

$$h_{\min}(t) \cong 2\pi fR|t| - h_0, \quad (5)$$

and the upper

$$h_{\max} = \infty. \quad (6)$$

The open profile is then

$$I(t) = \int_{h_{\min}(t)}^{\infty} f(z) dz = \frac{1}{2} \left\{ 1 - \text{erf}\left(\frac{h_{\min}(t)}{\sqrt{2}\sigma}\right) \right\} \\ \cong \frac{1}{2} \left[ 1 - \text{erf}\left(\frac{2\pi fR|t| - h_0}{\sqrt{2}\sigma}\right) \right]. \quad (7)$$

The tunnel-less and tunnel based chopper are compared in Fig. 4(c) with  $\sigma=0.025$  mm,  $h_0=0.075$  mm,  $R=100$  mm, and  $f=1000$  Hz. Note that the tunnel-less intensity goes gradually to zero. The base line is roughly twice of that for the tunnel. If an aperture  $s$  is added in front of the tunnel-less chopper, the open window becomes

$$I(t) = \begin{cases} \text{erf}\left(\frac{s}{2\sqrt{2}\sigma}\right) & \text{for } 0 \leq |t| \leq \frac{h_0 - s/2}{2\pi fR} \\ \frac{1}{2} \left\{ \text{erf}\left(\frac{s}{2\sqrt{2}\sigma}\right) - \text{erf}\left(\frac{-h_0 - 2\pi fR|t|}{\sqrt{2}\sigma}\right) \right\} & \text{for } \frac{h_0 - s/2}{2\pi fR} \leq |t| \leq \frac{h_0 + s/2}{2\pi fR} \end{cases} \quad (8)$$

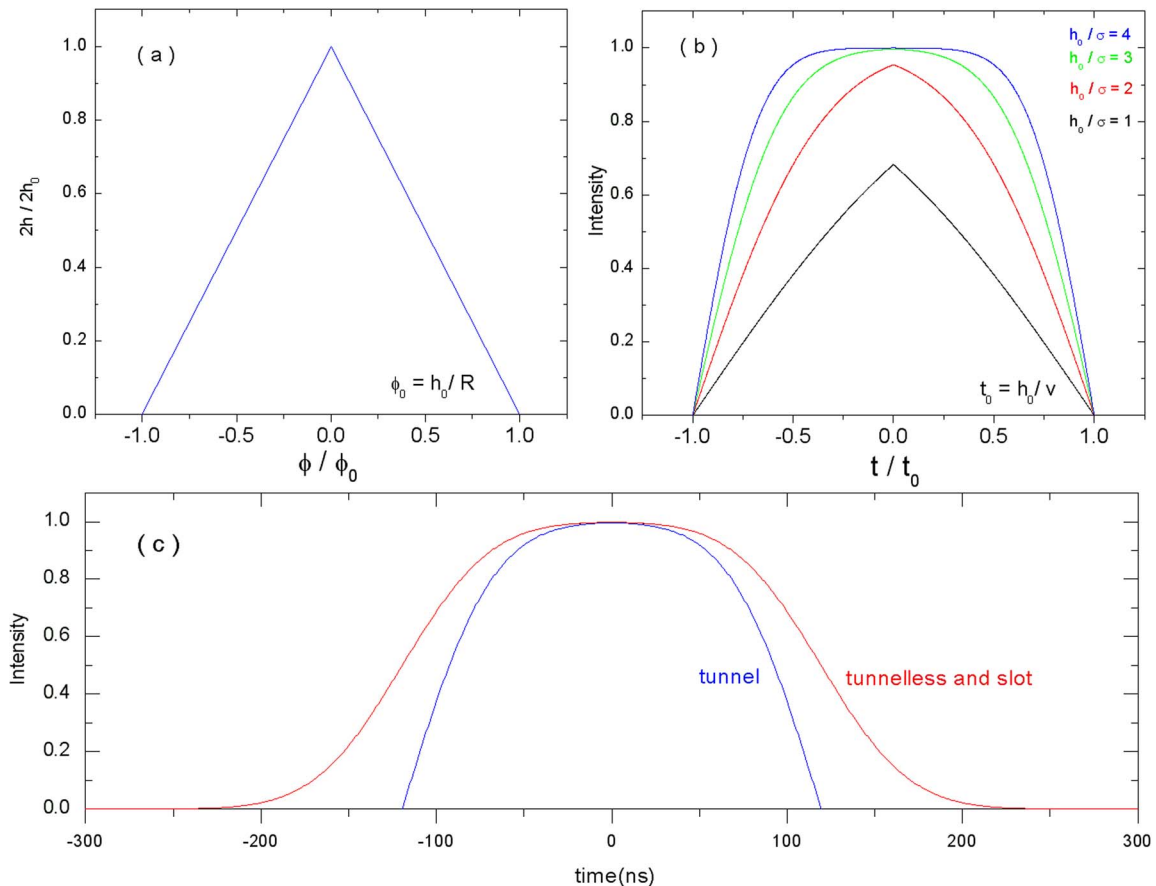


FIG. 4. (Color online) Chopper opening profiles: (a) the angle dependence of the tunnel aperture, (b) time-dependent intensity profile for beam/tunnel ratios of  $h_0/\sigma=1, 2, 3$ , and 4, and (c) comparison of time-dependent transmission for tunnel chopping vs tunnel-less and slotted wheel chopping. The parameters used in this comparison are  $\sigma=0.025$  mm,  $R=100$  mm,  $h_0=0.075$  mm, and  $f=1000$  Hz.

with  $I(t)=0$  for other times. The base line is determined by the condition that the two erf arguments are equal,

$$\Delta t_{\text{base}} = \frac{2h_0 + s}{2\pi fR}, \quad (9)$$

which is longer than the equivalent tunnel by the ratio  $(2h_0 + s)/2h_0$ . Pulse lengthening is thus the price to pay for tunable pulse length.

### C. Slot-based chopping

The integration limits for a small rotating slot with an aperture  $2h_0$  can be approximated by

$$h_{\text{min}}(t) \cong 2\pi fRt - h_0, \quad (10)$$

$$h_{\text{max}}(t) \cong 2\pi fRt + h_0, \quad (11)$$

which gives

$$I(t) = \int_{h_{\text{min}}(t)}^{h_{\text{max}}(t)} f(z) dz \cong \frac{1}{2} \left[ \text{erf} \left( \frac{2\pi fRt + h_0}{\sqrt{2}\sigma} \right) - \text{erf} \left( \frac{2\pi fRt - h_0}{\sqrt{2}\sigma} \right) \right]. \quad (12)$$

The rotating slot is essentially identical to the tunnel-less case for the same  $h_0$  as shown in Fig. 4(c). The advantage of the slot is the simplicity of machining many slots around the periphery. However as the periphery has to be thin to reduce the centrifugal pull on the rotation shaft, the absorption efficiency is lower than in the previous choppers where the pre- and postpulses hit the edges of the tunnel at normal incidence. The above formula is equivalent to the intensity of a slit scan in position across a Gaussian beam with a fixed gap  $2h_0$ . When the slit is much smaller than the beam, the scan measures the profile of the beam. In time space, that is the time it takes the radius to sweep across the beam. When the slit is much greater than the beam the scan measures the slit aperture.

A slot chopper is being built at Forschungszentrum Jülich for soft x rays at Bessy, Berlin. It has a radius of 170 mm and 1252 equidistant slots around the periphery. Each slot is 0.15 mm wide. Rotating at 998 Hz it produces 140 ns pulses at 1.25 MHz! The rim is only 0.5 mm thick to reduce the centrifugal force, so the absorption efficiency for x-ray beams has to be considered. Note that nuclear scattering experiments with microsecond isotopes could be done in 16-bunch mode with a slot chopper.

### IV. THE HIGH-SPEED CHOPPER

The ESRF high-speed chopper has a triangular titanium rotor which can be inscribed in a circle with radius of 96.8 mm. The vacuum chamber, the rotor, and the drawing of the beam positions are shown in Fig. 5. The rotation frequency is 986.3 Hz, the 360th subharmonic of the orbit frequency. The rotor has a tunnel on one of the three end-faces of the triangle. The tunnel is 165 mm long, 3 mm wide, and its height varies linearly from 0.10 to 0.22 mm across the width. The tunnel, which is semiopen, is formed by a channel with two 10 mm long roofs on the extremities. When the beam is

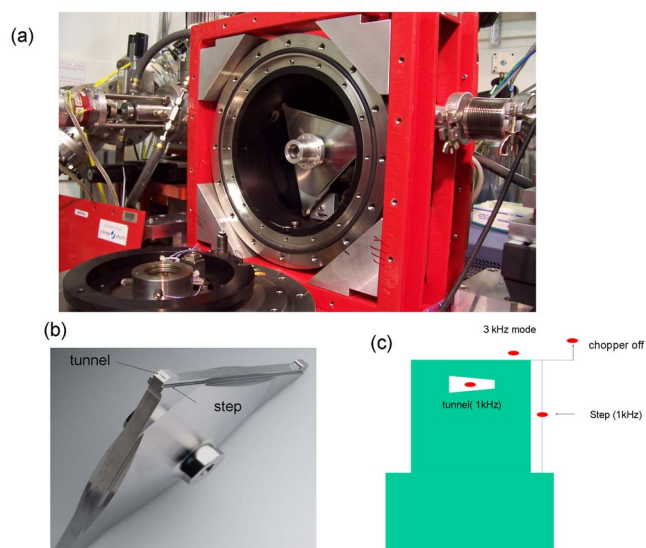


FIG. 5. (Color online) High-speed chopper. (a) Side view of triangular rotor in its vacuum chamber. The 20 mm thick walls of the stainless steel chamber provides safety and x-ray shielding. (b) Titanium rotor. Note the tunnel along one edge and the step used for tunnel-less chopping. (c) View of the trapezoidal tunnel, the steps alongside the tunnel, and different working positions for the x-ray beam (red).

chopped by the 0.10 mm part, the open base line is 192 ns. For the 0.22 mm part, it is 422 ns. When the beam is in the tunnel, the rotor opens once per turn. The rotor has two 5 mm deep steps on either sides of the tunnel as shown in Figs. 5(b) and 5(c). This allows making longer pulses up to 20  $\mu\text{s}$  by lowering the chopper relative to the beam without having to change the rotation frequency which simplifies the synchronization of a pump probe experiment. Note that the beam can also be positioned above the edges of the triangle where the rotor opens three times per revolution (3 kHz mode). The main parameters for the high-speed chopper are shown in Table I. We will discuss of the 3 kHz mode in Sec. IVB.

If the chopper is not needed during mirror alignment for example, it can be removed horizontally by moving the vacuum vessel by  $\sim 6.5$  mm (H). In this out position, the longer pulses from the heatload chopper become available (50–86  $\mu\text{s}$ ).

TABLE I. Chopper and ms-shutter parameters.

	Heat-load chopper	High-speed chopper	Millisecond shutter
Rotor shape	Circle	Triangle	Bar
Radius (mm)	75	96.8	30
Rotation frequency (Hz)	98.63	986.3	2.681
Pulse frequency (Hz)	986.3	986.3	0–80
Tip speed (m/s)	46.5	599.8	0.51
Tunnel height (mm)	4.0	0.10–0.22	0.3–4.0
Tunnel width $w$ (mm)	8.0	3.0	5.0
Tunnel length (mm)	150.0	167.7	60.0
$\Delta t_{\text{base\_tunnel}}$ ( $\mu\text{s}$ )	85	0.19–0.42	600–4000
Step height (mm)	0.45–1.65	5.0	...
$\Delta t_{\text{base\_step}}$ ( $\mu\text{s}$ )	34–86	0–20	...
Rotation jitter ( $\mu\text{s}$ ; rms)	2	0.003	50

One advantage of a triangular rotor geometry is that the tunnel is off axis. That makes it easier to taper the rotor in the radial direction to increase the mechanical strength near the rotation axis where the centrifugal stress accumulates. A slight drawback of the triangle is the lower vertical speed, which is reduced by  $\cos(30^\circ) = \sqrt{3}/2 = 0.866$  for the triangle. The tangential speed is 599.8 m/s (1.7 times the speed of sound in air) and the vertical speed 519.4 m/s. As a consequence, the base line in the open window for the triangular tunnel takes the form

$$\Delta t_{\text{base}} = \frac{2h_0}{\sqrt{3}\pi f R}. \quad (13)$$

The chopper is installed in the (quasi) focused beam 1.2 m from the sample where the beam is small which improves the chopping efficiency. The beam size in the tunnel is 0.37 mm (H)  $\times$  0.07 mm (V), which converges to 0.10 mm (H)  $\times$  0.06 mm (V) in the focus (FWHM). As the beam is small horizontally compared to the 3 mm wide tunnel, the height of the tunnel that cuts the beam can be varied from 0.10 to 0.22 mm by translating the chopper horizontally.

The phase locking of the high-speed chopper is done with a pickup signal from a small magnet integrated in the rotor. This signal is compared with a time to live (TTL) reference signal at 986.3 Hz, which is a frequency divided (360) and phase shifted copy of the orbit clock. The time delay of the TTL signal can be delayed to a resolution of 5.6 ns, which is sufficient for centering the open window onto one pulse. The internal clock in the chopper controller runs at 352 MHz and the pickup signal is measured to 2.8 ns (rms) resolution. The measured rotation jitter is 2.8 ns (rms) depending on the mechanical vibrations around the chopper.

In the direction of the beam, the high-speed chopper is followed by a slit that adjusts the beam size on the sample. If the vertical slit is smaller than the tunnel height, the (cw) open profile becomes trapezoidal in shape. In the central part, the open profile is constant for a time and the top line of the open window is

$$\Delta t_{\text{top}}(\text{tunnel}) = \frac{2h_0 - s}{\sqrt{3}\pi f R}. \quad (14)$$

The base line is

$$\Delta t_{\text{base}}(\text{tunnel}) = \frac{2h_0}{\sqrt{3}\pi f R}. \quad (15)$$

The equivalent expressions for the tunnel-less case are

$$\Delta t_{\text{top}}(\text{tunnel-less}) = \frac{2h_0 - s}{\sqrt{3}\pi f R} \quad (16)$$

and

$$\Delta t_{\text{base}}(\text{tunnel-less}) = \frac{2h_0 + s}{\sqrt{3}\pi f R}. \quad (17)$$

These open windows are shown schematically in Fig. 6. Note that the top line is the same in the two cases, but that the tunnel-less base line is prolonged by  $(2h_0 + s)/2h_0$  as for a full Gaussian beam.

We will now compare the open times for tunnel and tunnel-less chopping in the 16-bunch mode, the most demanding chopper mode but also the most frequent mode for single pulse experiments. In 16 bunch mode the pulses are separated by 176 ns. With  $2h_0 = 0.12$  mm,  $R = 96.8$  mm,  $f = 986.3$  Hz, and a vertical slit  $s = 0.06$  mm, we get  $\Delta t_{\text{top}} = 116$  ns and  $\Delta t_{\text{base}} = 231$  ns. If the open window is centered on the pulse, the pulse will pass the tunnel with a clearance to the walls of only 0.03 mm. Moreover the pre- and post-pulses are 61 ns from the edges of the open window, which is much greater than the 2.8 ns (rms) rotation jitter. The side pulses are thus perfectly blocked. In addition the 116 ns long top line, compared with the 2.8 ns (rms) rotation jitter, ensures a high pulse to pulse stability, which is particularly important for scanning diffraction experiments. In the equivalent tunnel-less case with  $h_0 = 0.06$  mm, the base line is 347 ns and the top line 116 ns. The distance to the side pulses is 2.5 ns, which is insufficient in view of the 2.8 ns (rms) rotation jitter. Raising the chopper to  $h_0 = 0.05$  mm, we get  $\Delta t_{\text{base}} = 308$  ns and  $\Delta t_{\text{top}} = 77$  ns, which increases the side pulse clearance to 22 ns, which is fine. Finally a long pulse is obtained for  $h_0 = 2.5$  mm, which gives a nearly rectangular pulse shape with  $\Delta t_{\text{base}} = 9.74$   $\mu\text{s}$  and  $\Delta t_{\text{top}} = 9.51$   $\mu\text{s}$ .

### A. Tunnel-less chopping at 3 kHz

The high-speed chopper is mainly designed to produce pulses at 1 kHz, which, compared to the 5.7 MHz frequency of a 16-bunch beam, makes extremely poor use of the beam. In liquid experiments where the sample can be exchanged rapidly in a jet, it would be advantageous to run at higher frequencies. Rotating the chopper above 1000 Hz is not possible with the present rotor due to a resonant shaft-bending mode at 1100 Hz, followed by centrifugal fracture at 1450 Hz. The simplest option is to use the three sides of the rotor in tunnel-less mode with the beam outside the rotor and in a lateral position where it never hits the tunnel [see Fig. 5(c)]. This poses the following challenge: the rotor spins around its center of mass, which, due to finite tolerances, differs slightly from the geometrical center. Is the rotor machined and balanced well enough to isolate single pulses in the 16-bunch mode at 3 kHz? The challenge is to get the same open window from the three sides, i.e., that the beam heights  $h_0$ , for the three sides are sufficiently identical that the open windows select one pulse only and that they arrive at the right time. The rotor turns in the clockwise direction and face 1 is the one with the tunnel and faces 2 and 3 follow in time. We find faces 2 and 3 to be 16 and 19  $\mu\text{m}$  closer to the beam than face 1, respectively. Moreover the angles in the triangle have to be  $60^\circ$  to avoid systematic shifts in the time position of the open window. For example, with an angular speed of 0.355 mdeg/ns at 986.3 Hz, it follows that if one rotor angle is 3.55 mdeg too big, the associated open window will arrive 10 ns too late. By tracing the open profiles in time from the three faces, the three angles were measured to be  $59.998(1)^\circ$ ,  $60.003(1)^\circ$ , and  $59.999(1)^\circ$ , which is just sufficient for 3 kHz operation (see below).

We saw previously that single pulse selection in tunnel-less typically requires  $h_0 = 0.05$  mm and  $s = 0.06$  mm. So the

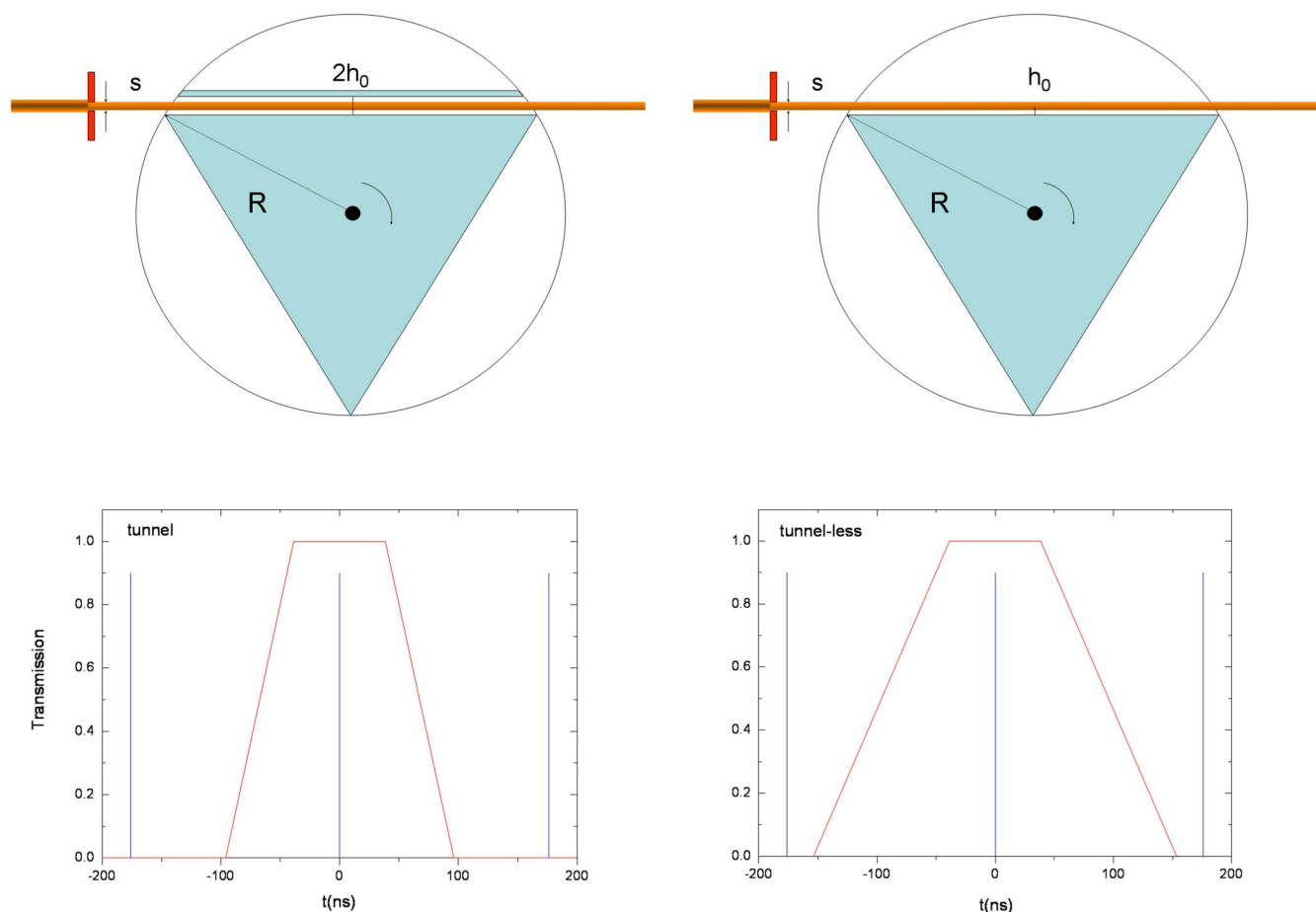


FIG. 6. (Color online) Beam positions and corresponding trapezoidal open windows for the high-speed chopper. The tunnel mode is shown on the left and the tunnel-less mode on the right. The open profiles are for  $h_0=s=0.06$  mm. The chopper is capable of isolating a single pulse out of the 16-bunch pulse train (176 ns separation) with both tunnel and tunnel-less chopping modes.

beam distance to the floor is only 0.02 mm. A quick estimate shows that  $h_0$  can vary between 0.03 and 0.05 mm in single pulse mode. The lower limit is imposed by intensity conservation and the upper by side-pulse discrimination.

We characterized the 3 kHz pulse train with a continuous cw beam.  $h_0$  was moved to 0.05 mm on the tunnel side (side 1) and the slit was  $s=0.06$  mm. This gives a 308 ns base line, which is fine for the 16-bunch mode. The open window was measured with a Cyberstar scintillation detector coupled to a 6 GHz oscilloscope (LeCroy 6 GHz, WaveMaster6820A). The pulse train is shown on the millisecond scale in Fig. 7(a) and with a nanosecond zoom in Fig. 7(b). The pulse in the middle (pulse 3) is from face 1 with the tunnel and pulses 1 & 4 and 2 & 5 are produced by face 2 and 3, respectively. In Fig. 7(b) the nanosecond open profiles are offset in time by 0, 1/3, and 2/3 of the principal revolution time of the rotor. Note that pulse 3 is trapezoidal and we use that pulse to define time zero. In contrast, pulse 1 (4) and 2 (5) are triangular, slightly shorter, and shifted in time by a few nanoseconds (see Table II). That means that the associated rotor sides are closer to the beam and their angles differ slightly from  $60^\circ$ .

We conclude that 3 kHz single pulse selection is possible in 16-bunch mode, but the margins in space and time are very tight for routine operation. Note that the rising edge of

pulse 1 is 10 ns from the prepulse at  $-176$  ns. This means that the phase of the rotor has to be stable to 10 ns over the duration of an experiment, which might run for several days.

A future rotor could have a bigger radius (150 mm) while thinning the tips from 6 to 2 mm to minimize the centrifugal stress on the rotation shaft. With this rotor at 986.3 Hz, the settings for single pulse selection in 16-bunch mode would be  $h_0=0.09$  mm,  $s=0.06$  mm,  $\Delta t_{\text{base}}=298$  ns, and  $\Delta t_{\text{top}}=231$  ns. The distance to the satellite pulses would be 27 ns, i.e., about ten times the rms jitter and therefore safe. Also if the tunnel height varies between 0.10 and 0.22 mm, the base lines will vary from 128 to 295 ns. Alternatively the tunnel could be 50% higher and accept larger beams.

## V. THE HEATLOAD CHOPPER

The first white beam experiments were done without a heatload chopper, which meant that the high-speed chopper had to withstand 60–120 W of power from the focused white beam during exposure of the detector. Because a rotor in magnetic bearings is only cooled by radiation, it was necessary to reduce the beam power by closing down the aperture of the primary slits and reducing the power of the undulator by opening the gap to about 9 mm rather than using the full

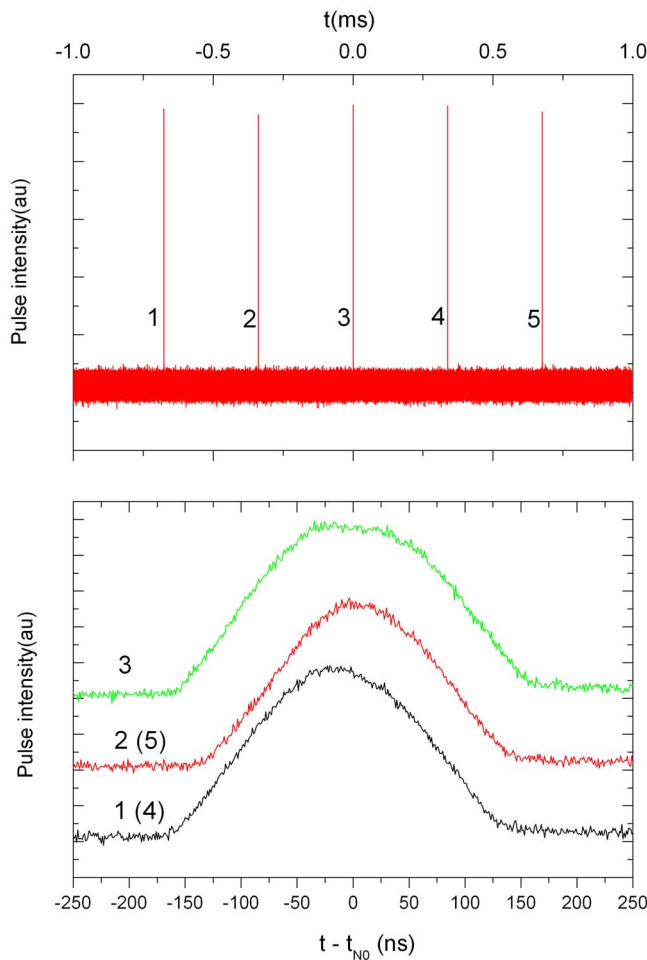


FIG. 7. (Color online) Transmission of the high-speed chopper when operated in 3 kHz tunnel-less chopping mode (recorded with a cw beam). (a) Pulse train on the millisecond time scale. (b) Time-dependent transmission from the three faces of the triangle is superimposed by shifting each by  $t_{No}$  (theoretical arrival time for pulse  $N$  given a perfect equilateral rotor).

power position at 6 mm. In practice the total power was reduced by a factor 6 to avoid overheating the high-speed rotor with a similar reduction in peak intensity of the pulses. The solution was to install a water cooled heatload chopper upstream the monochromator and mirror in the optics hutch.

The heatload chopper is a Cu disk that rotates in vacuum about a horizontal axis perpendicular to the beam. The radius of the disk is 75 mm and the disk has five tunnels (see Fig. 8). The tunnels are 4 mm high, 8 mm wide, and 150 mm long. The size of the beam in the heatload chopper is up to 7 mm (H)  $\times$  0.7 mm (V). Normally the disk rotates at 98.63 Hz at the 3600 subharmonic of the orbit frequency, i.e. ten times slower than the high-speed chopper, but it can also

TABLE II. Pulse parameters for the principal pulses from the high-speed chopper in 3 kHz mode.

Pulse	$\Delta t_{\text{base}}$ (ns)	$\Delta t_0$ (ns)	$h$ (mm)
1	295	-12.7	0.047
2	270	5.4	0.04
3	317	0	0.052

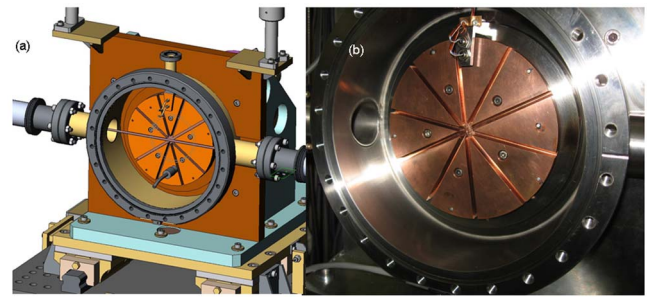


FIG. 8. (Color online) Heatload chopper. (a) Drawing of chopper rotor in its vacuum vessel. The position of the chopper relative to the x-ray beam is optimized by motorized translation in the vertical and horizontal directions. (b) Photo of the five-tunnel rotor in its vacuum vessel. The rotor position is sensed by a coil located near the top of the photo. This coil generates a current pulse when SmCo pickup magnets pass by (seen as gray dots near the periphery of the rotor).

rotate at any subharmonic between 3 and 98.63 Hz. As the five tunnels open ten times per revolution, the heatload chopper produces pulses at 986.3 Hz in phase with the high-speed chopper. The chopper parameters are listed in Table I. The vertical beam size is smaller than the tunnel height, which makes the temporal open profile trapezoidal with

$$\Delta t_{\text{top}}(\text{tunnel}) = \frac{2h_0 - s}{2\pi fR} \quad (18)$$

and

$$\Delta t_{\text{base}}(\text{tunnel}) = \frac{2h_0}{2\pi fR}. \quad (19)$$

The denominator in Eqs. (18) and (19) is the vertical speed at the end of the tunnels. With  $2h_0=4$  mm,  $s=0.7$  mm,  $R=75$  mm, and  $f=98.63$  Hz, we get  $v=46.5$  m/s,  $\Delta t_{\text{top}}=71.0$   $\mu\text{s}$ , and  $\Delta t_{\text{base}}=86.0$   $\mu\text{s}$ . By integrating the trapezoidal in time, we get the duty cycle of the chopped beam

$$D = N \frac{\left(2h_0 - \frac{s}{2}\right)}{\pi R}, \quad (20)$$

where  $N$  is the number of tunnels. For  $N=5$ , we get  $D=0.077$ , which gives a heatload reduction of  $D^{-1}=12.9$ . For a typical white beam in 16-bunch mode at 90 mA, the heatload chopper reduces the power from 62 to 4.8 W, which (still) raises the temperature of the high-speed chopper from 20 to 45  $^{\circ}\text{C}$ .

The tunnel height  $2h_0$  in the heatload chopper was chosen to be big (4 mm) to have margins for rotation jitter, which was expected to be as high as 10  $\mu\text{s}$  (rms) due to the mechanical bearings and the flow of cooling water in the rotation shaft. A 70  $\mu\text{s}$  top line is compatible with a jitter of 10  $\mu\text{s}$  (rms) without cutting the central part of the pulse. The measured jitter at 100 Hz is 2  $\mu\text{s}$  so the tunnel height could be reduced in future designs. At 10 Hz the jitter increases to 50  $\mu\text{s}$  and at 3 Hz, the lowest possible speed, the jitter is 200  $\mu\text{s}$ .

The low jitter at 100 Hz makes it more efficient to run the heatload chopper in tunnel-less mode with a small distance  $h_0$  to the tunnel floor. By adapting Eqs. (16) and (17) to

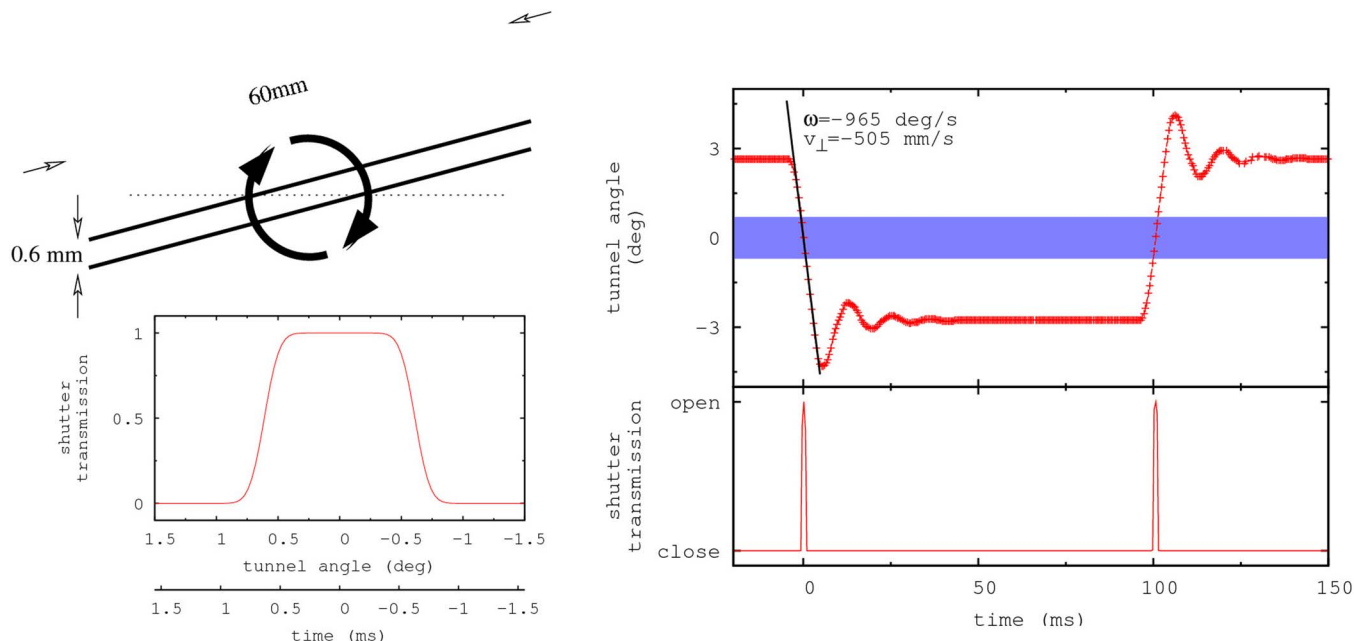


FIG. 9. (Color online) Millisecond shutter. (a) Geometric parameters for the tunnel. (b) Tunnel transmission as a function of angle and time. (c) Time-dependent angular position of the tunnel (top) when operating the shutter at 10 Hz. The tunnel transmits a 1.4 ms pulse each time it toggles back and forth over a  $6^\circ$  range. Higher acceleration will be needed to isolate a single pulse when operating the high-speed chopper in the 3 kHz mode.

a tunnel-less disk with  $h_0=1$  mm,  $s=0.7$  mm,  $R=75$  mm, and  $f=98.63$  Hz, we get  $\Delta t_{\text{op}}=28.0$   $\mu\text{s}$  and  $\Delta t_{\text{base}}=58.1$   $\mu\text{s}$ . The duty cycle is

$$D = N \frac{2h}{\pi R}, \quad (21)$$

which gives  $D=0.042$  and a heat reduction of  $D^{-1}=23.6$ . This mode is realized by shifting the chopper 1 mm vertically, which leaves 0.65 mm clearance to the floor when the tunnel is fully open. That distance is ten times greater than machining and balancing errors in the tunnel positions and therefore is a good working point.

The Cu disk is driven by a synchronous direct drive motor in air. The vacuum passage is a ferrofluidic feed through with cooling water running in the rotation axis. The disk is cooled from one side by a stainless steel flange, which is attached to the ferrofluid feed through. Theoretically, the heatload chopper can absorb 450 W with a temperature rise of 104 K (1.3 K in the cooling water). The disk temperature is measured by a Raytech infrared detector. The detector shows higher temperatures than expected, which indicates a poor heat transfer between the cold flange and the disk. We plan to improve this by explosion melting the stainless steel flange onto the Cu disk, which seems the best way to bond two different metals together in a water-leak-tight fashion under UHV conditions.

The disk is dynamically balanced at 100 Hz to minimize eccentricity and friction in the bearings. The rotation speed is synchronized using a pickup signal from a SmCo magnet on the disk. In the first version of the heatload chopper, the magnet was made of NdFeB, but it demagnetized at temperatures around 150  $^\circ\text{C}$ . The new SmCo magnet is weaker (20 mT), but it maintains its magnetization up to 250  $^\circ\text{C}$ . By comparing the difference between the pickup and a phase

shifted TTL at 98.63 Hz, the disk is either accelerated or decelerated until the two signals coincide within the time resolution of the controller (11.3 ns,  $rf/8$ ).

The vacuum vessel of the heatload chopper is motorized in the horizontal and vertical positions. The tunnel is 8 mm wide and receives a 7 mm wide beam. When not used, the heatload chopper is moved 8 mm horizontally toward the synchrotron.

We finally note that the heatload chopper is readily modified for 3 kHz operation by increasing the number of tunnels from 5 to 15. Also if the tunnel height is reduced from 4.0 to 1.33 mm, the heatload reduction remains the same as at present.

## VI. THE MILLISECOND SHUTTER

Many pump-probe experiments cannot run at the default 986.3 Hz chopper frequency due to heatload from the laser or the presence of slower-time-scale kinetics in the sample. Hence, a millisecond shutter is needed to lower the pulse frequency on the sample. The millisecond shutter is installed in vacuum just before the high-speed chopper. The shutter is water cooled via its ferro-fluid feed-through to the stepper motor in air. The millisecond shutter can be seen upstream the high-speed chopper in Fig. 5

The millisecond shutter is a rotating tunnel which is wire cut from a  $60 \times 8.5 \times 4$  mm<sup>3</sup> block of tungsten carbide. The tunnel is 60 mm long, 5 mm wide, and the tunnel height increases from 0.3 which gives the tunnel a trapezoidal cross section. As the beam is small in the millisecond shutter, 0.40 mm (H)  $\times$  0.07 mm (V), the open time can be changed by moving the shutter horizontally without changing other parameters (motor speed and delay). The bar is mounted on a rotation axis driven by a high-speed stepper motor (PV267-D2.8BA, Oriental Motor). To optimize the

speed of the stepper motor, the angular step size is rather coarse with  $0.9^\circ$  per step. When working with a 0.6 mm tunnel, the tunnel is already closed when the shutter is rotated by  $\pm 0.6^\circ$ , i.e., the shutter is only open for one single position of the motor. At full speed, the angular speed is  $965^\circ/\text{s}$  ( $f=2.681$  Hz). The open time can be calculated with the heatload chopper formulas (18) and (19), with  $R=30$  mm. The base line open window is 0.6 ms for  $2h_0=0.3$  mm and 4.0 ms for  $2h_0=2.0$  mm (see Table I).

In the pulsed mode the shutter is operated in the following way. In its close position, the tunnel angle is rotated  $+2.7^\circ$  away from the beam direction, which is three steps from the open position [see Fig. 9(a)]. The shutter opens “on the fly” by moving the tunnel to  $-2.7^\circ$ . The motion of the shutter is monitored by a 2000 step/turn linear encoder as shown in Fig. 9(b). Note that the shutter does not stop perfectly at  $-2.7^\circ$ ; it overshoots slightly but settles quickly at the correct value after 2–3 small oscillations without crossing the open region  $\pm 0.6$  deg while settling down. The amplitude of the “overshoots” was reduced by mounting a damper on the stepper motor. The millisecond shutter is phased in time with the chopper pulse using a TTL signal derived from the timing module to start the execution of a program in the motor driver card. By carefully optimizing the current in the motor, the close/open/close cycle can be repeated at 80 Hz without losing steps.

## VII. CONCLUSION AND OUTLOOK

The chopper system for pump-probe experiments on ID09B has been presented together with the bunch structures for single pulse experiments at the ESRF. The use of high brightness white beams is now possible, thanks to a heatload chopper that reduces the thermal load on downstream elements by a factor of around 20. In default mode the two choppers produce pulses at 1 kHz, but they can also be configured at other subharmonics of the orbit frequency between 0 and 3 kHz. With the high-speed chopper in tunnel mode, open times as short as 200 ns can be obtained with a jitter of 2.8 ns (rms). That is short enough to isolate single pulses of x rays from all timing modes at the ESRF. The shortest x-ray pulse is 60 ps long and produced by a low bunch charge in the 7/8 mode. Longer pulses train up to 20  $\mu\text{s}$  can be made by the step on the high-speed chopper or by the heatload chopper alone (86  $\mu\text{s}$ ). Finally a pulsed millisecond shutter is used to lower the frequency of the experiments from 80 Hz to single shot.

The prospect of running experiments at 3 kHz is demonstrated with the existing triangular rotor in the high-speed chopper. In general the high frequency option might be useful for lower electron energy synchrotrons between 2 and 3 GeV to compensate for their lower brightness above 10 keV. Likewise at the ESRF with 6 GeV electrons, a 3 kHz option might compensate for the loss of intensity from undulators

above 20 keV and compensate for losses associated with the use of multilayer optics to control the bandwidth of the white beam.

## ACKNOWLEDGMENTS

We would like to thank Wilfried Schildkamp, Claude Pradervand, Keith Moffat, Dominique Bourgeois, Thomas Ursby, Loys Goirand, Jean-Luc Revol, Roland Taffut, Herve Gonzales, and Ernesto Paisier for their contributions to this project.

- <sup>1</sup>V. Šrajer, T. Teng, T. Ursby, C. Pradervand, Z. Ren, S. Adachi, W. Schildkamp, D. Bourgeois, M. Wulff, and K. Moffat, *Science* **274**, 1726 (1996).
- <sup>2</sup>B. Perman, V. Šrajer, Z. Ren, T.-Y. Teng, C. Pradervand, T. Ursby, F. Schotte, M. Wulff, R. Kort, K. Hellingwerf, and K. Moffat, *Science* **279**, 1946 (1998).
- <sup>3</sup>D. Bourgeois, B. Vallone, F. Schotte, P. Anfinrud, M. Wulff, and M. Brunori, *Proc. Natl. Acad. Sci. U.S.A.* **100**, 8704 (2003).
- <sup>4</sup>H. Ihee, S. Rajagopal, V. Šrajer, R. Pahl, S. Anderson, M. Schmidt, F. Schotte, P. A. Anfinrud, M. Wulff, and K. Moffat, *Proc. Natl. Acad. Sci. U.S.A.* **102**, 7145 (2005).
- <sup>5</sup>M. Cammarata, M. Levantino, F. Schotte, P. A. Anfinrud, F. Ewald, J. Choi, A. Cupane, M. Wulff, and H. Ihee, *Nat. Methods* **5**, 10 (2008).
- <sup>6</sup>A. Plech, M. Wulff, S. Bratos, F. Mirloup, R. Vuilleumier, F. Schotte, and P. A. Anfinrud, *Phys. Rev. Lett.* **92**, 125505 (2004).
- <sup>7</sup>H. Ihee, M. Lorenc, T. K. Kim, Q. Y. Kong, M. Cammarata, J. H. Lee, S. Bratos, and M. Wulff, *Science* **309**, 1223 (2005).
- <sup>8</sup>T. K. Kim, M. Lorenc, J. H. Lee, M. Lo Russo, J. Kim, M. Cammarata, Q. Kong, S. Noel, A. Plech, M. Wulff, and H. Ihee, *Proc. Natl. Acad. Sci. U.S.A.* **103**, 9410 (2006).
- <sup>9</sup>J. Davidsson, J. Poulsen, M. Cammarata, P. Georgiou, R. Wouts, G. Katona, F. Jacobson, A. Plech, M. Wulff, G. Nyman, and R. Neutze, *Phys. Rev. Lett.* **94**, 245503 (2005).
- <sup>10</sup>M. Wulff, S. Bratos, A. Plech, R. Vuilleumier, F. Mirloup, M. Lorenc, Q. Kong, and H. Ihee, *J. Chem. Phys.* **124**, 034501 (2006).
- <sup>11</sup>M. Cammarata, M. Lorenc, T. K. Kim, J. H. Lee, Q. Y. Kong, E. Pontecorvo, M. Lo Russo, G. Schiró, A. Cupane, M. Wulff, and H. Ihee, *J. Chem. Phys.* **124**, 124504 (2006).
- <sup>12</sup>A. D. LeGrand, W. Schildkamp, and B. Blank, *Nucl. Instrum. Methods Phys. Res. A* **275**, 442 (1989).
- <sup>13</sup>D. Bourgeois, T. Ursby, M. Wulff, C. Pradervand, A. Legrad, W. Schildkamp, S. Labouré, V. Šrajer, T. Y. Teng, M. Roth, and K. Moffat, *J. Synchrotron Radiat.* **3**, 65 (1996).
- <sup>14</sup>D. Kosciesza and H. Bartunik, *J. Synchrotron Radiat.* **6**, 947 (1999).
- <sup>15</sup>A. McPherson, J. Wang, P. L. Lee, and D. M. Mills, *J. Synchrotron Radiat.* **7**, 1 (2000).
- <sup>16</sup>A. McPherson, W.-K. Lee, and D. Mills, *Rev. Sci. Instrum.* **73**, 2852 (2002).
- <sup>17</sup>M. Gembicky, D. Oss, R. Fuchs, and P. Coppens, *J. Synchrotron Radiat.* **12**, 665 (2005).
- <sup>18</sup>M. Gembicky, S. Adachi, and P. Coppens, *J. Synchrotron Radiat.* **14**, 295 (2007).
- <sup>19</sup>S. Nozawa, S. Adachi, J. Takahashi, R. Tazaki, L. Guerin, M. Daimon, A. Tomita, T. Sato, M. Chollet, E. Collet, H. Cailleau, S. Yamamoto, K. Tsuchiya, T. Shioya, H. Sasaki, T. Mori, K. Ichiyangi, H. Sawa, H. Kawata, and S. Koshihara, *J. Synchrotron Radiat.* **14**, 313 (2007).
- <sup>20</sup>M. Wulff, A. Plech, L. Eybert, R. Randler, F. Schotte, and P. Anfinrud, *Faraday Discuss.* **122**, 13 (2003).
- <sup>21</sup>F. Schotte, S. Teichert, P. A. Anfinrud, V. Šrajer, K. Moffat, and M. Wulff, in *Third-Generation Hard X-ray Synchrotron Radiation Sources*, edited by D. Mills (Wiley, New York, 2002), pp. 345–401.
- <sup>22</sup>B. Lindenau, J. Raebiger, S. Polachowski, and J. K. Fremerey, *AIP Conf. Proc.* **705**, 1019 (2004).